Experimental Limits on Exotic Spin and Velocity Dependent Interactions Using Rotationally Modulated Source Masses and an Atomic-Magnetometer Array

K. Y. Wu, S. Y. Chen, G. A. Sun, S. M. Peng, and M. Peng
Institute of Nuclear Physics and Chemistry, CAEP, Mianyang, Sichuan 621900, China

H. Yan*
Key Laboratory of Neutron Physics, Institute of Nuclear Physics and Chemistry, CAEP, Mianyang, Sichuan 621900, China and Institute of Nuclear Physics and Chemistry, CAEP, Mianyang, Sichuan 621900, China

(Received 28 September 2021; accepted 7 July 2022; published 29 July 2022)

Various theories beyond the standard model predict new interactions mediated by new light particles with very weak couplings to ordinary matter. Interactions between polarized electrons and unpolarized nucleons proportional to $g_V^N g_A^e \vec{\sigma}\cdot\vec{v}$ and $g_A^N g_A^e \vec{\sigma}\cdot\vec{v}\times\vec{r}$ are two such examples, where $\vec{\sigma}$ is the spin of the electrons, $\vec{r}$ and $\vec{v}$ are position and relative velocity between the polarized electrons and nucleons, g_V^N/g_A^N is the vector or axial-vector coupling constant of the nucleon, and g_A^e is the axial-vector coupling constant of the electron. Such interactions involving a vector or axial-vector coupling g_V^N/g_A^N at one vertex and an axial-vector coupling g_A^e at the polarized electron vertex can be induced by the exchange of spin-1 bosons. We report new experimental upper limits on such exotic spin-velocity-dependent interactions of the electron with nucleons from dedicated experiments based on a recently proposed scheme. We rotationally modulated two ~6 Kg source masses at a frequency of 20 Hz. We used four identical atomic magnetometers in an array form to increase the statistics and cancel the common-mode noise. We applied a data processing method based on high precision numerical integration for the four harmonic frequencies of the signal. We reverse the rotation direction of the source masses to flip the signal due to the new interactions; thus, we can apply the $[+1,-3,+3,-1]$ weighting method to remove possible slow drifting. Our constraint on the product of vector and axial-vector couplings is $|g_V^N g_A^e| < 2.1\times10^{-34}$ and on the product of axial-vector and axial-vector couplings is $|g_A^N g_A^e| < 2.4\times10^{-22}$ for an interaction range of 10 m. The new constraints on vector-axial-vector interaction improved by as much as more than 4 orders of magnitude and on axial-axial interaction by as much as 2 orders of magnitude in the corresponding interaction range, respectively.

DOI: 10.1103/PhysRevLett.129.051802

Introduction.—New interactions mediated by new particles are solutions to several important questions in modern physics, such as the strong CP(Charge-conjugation Parity symmetry) problem [1] and dark matter [2]. Long ago, Peccei and Quinn [3] proposed the PQ mechanism to solve the strong CP problem. Wilczek [4] and Weinberg [5] simultaneously noticed the PQ mechanism would generate new pseudoscalar particles, which are named axions. In 1984, Moody and Wilczek [6] pointed out that ALPs (axionlike particles) could mediate macroscopic spin-dependent interactions. Many experiments have been performed to search for and constrain the scalar-pseudoscalar type of interaction [7–13]. Later on, starting from rotational invariance, Dobrescu and Mocioiu [14] formed 16 different operator structures involving the spin and momenta of the interacting particles. ALPs mediated new interactions are a subset of the new theory. Now the interaction carriers could also be vector particles such as the paraphoton (dark, hidden, heavy, or secluded photon) [15,16], Z' boson [2], graviphoton [17], etc.

For the vector interaction carriers, the interaction can be deduced from the coupling $\mathcal{L}_X = \bar{\psi}(g_V\gamma^\mu + g_A\gamma^\mu\gamma_5)\psi X_\mu$ where X_μ is the new vector particle and g_V and g_A are the vector and axial coupling constants [18–22]. We can express the VA (vector-axial-vector) interaction $V_{\mathrm{VA}}(r)$ ($V_{12,13}$ in Ref. [14]'s notation) and AA(axial-axial) interaction $V_{\mathrm{AA}}(r)$ ($V_{4,5}$ in Ref. [14]'s notation) as

$$V_{\mathrm{VA}}(r) = \frac{\hbar g_V g_A}{4\pi}\frac{\exp(-r/\lambda)}{r}\vec{\sigma}\cdot\vec{v}, \tag{1}$$

$$V_{\mathrm{AA}}(r) = \frac{\hbar^2 g_A^2}{16\pi mc}\left(\frac{1}{\lambda r}+\frac{1}{r^2}\right)\exp(-r/\lambda)\vec{\sigma}\cdot(\vec{v}\times\hat{r}), \tag{2}$$

where $\vec{v}$ is the relative velocity between the probe particle and source particle, $\lambda = \hbar/m_X c$ is the interaction range, m_X is the mass of the new vector boson, m is the mass, and $\vec{\sigma}$

are the Pauli matrices of the spin-polarized probing particle. $g_V g_A$ and $g_A g_A$ are the interaction coupling constants that are both dimensionless.

Many experiments have been carried out to scan a significant amount of parameter space for ALPs, which have eluded detection. Since these new light bosons can mediate macroscopic interactions, one method to search for these new particles is to probe the boson field induced by a macroscopic body [21–32]. Reference [32] is an extensive review of recent theoretical and experimental progress of research on the new interaction search.

Because of its high sensitivity (Subfemtotesla sensitivity has been reported in Ref. [33].) based on polarized electron spins [34], AMs(atomic magnetometers) are convenient for searching for these exotic new spin-dependent interactions. Chu *et al.* first proposed to use a commercially available AM to detect the new interactions [35]. Then Kim *et al.* employed a commercial cm-scale AM to search for the interaction between polarized valence electrons of Rb in the vapor cell of the magnetometer and nucleons [25,26]. The commercially available AMs have relatively low sensitivities but are more compact and can be easily arranged in an array of 50 units to measure the biomagnetic field generated by the human brain [36–38]. To the best of our knowledge, the AMs in the array form have never been used to search for spin-dependent new interactions.

Inspired by using the compact AM in new interaction searches [25,26,35] and utilizing an array of AMs to measure the biomagnetic field [36–38], in Ref. [39], we proposed to use rotationally modulated source masses and an array of AMs to search for the exotic spin-dependent interactions.We follow the previously proposed scheme to search for the VA and AA type of new interactions in this Letter.

The basic idea.—We first briefly review the basic idea of the previously proposed experiment scheme [39]. Two dense, identical source masses are rotationally modulated at frequency f_0. An array consisting of four identical AMs is placed symmetrically around the source masses. If the exotic spin-dependent interactions exist, a pseudomagnetic field can be induced by the source masses. Now the probing polarized particle is assumed to be the electron since the AM is using polarized electrons. Taking $g_V g_A = g_A^2 = 1$, at the position of the AM, we can calculate the pseudomagnetic field B' induced by VA and AA interactions by integrating Eqs. (1) and (2), respectively. Theoretically, the pseudomagnetic field at the point $\vec{r}$ can be calculated and expressed as

$$\vec{B}'_{\mathrm{VA}}(\vec{r}) = \frac{g_V g_A \rho_N}{2\pi\gamma_e} \int d^3\vec{r}' \frac{\exp\left(-|\vec{r}-\vec{r}'|/\lambda\right)}{|\vec{r}-\vec{r}'|} \vec{v},$$

$$\vec{B}'_{\mathrm{AA}}(\vec{r}) = \frac{\hbar g_A^2 \rho_N}{8\pi m_e c \gamma_e} \int d^3\vec{r}' \left(\frac{1}{\lambda|\vec{r}-\vec{r}'|} + \frac{1}{|\vec{r}-\vec{r}'|^2}\right) \times \exp\left(-|\vec{r}-\vec{r}'|/\lambda\right)\left(\vec{v} \times \frac{\vec{r}-\vec{r}'}{|\vec{r}-\vec{r}'|}\right),$$

where γ_e is the gyromagnetic ratio of the electron, ρ_N is the nucleon number density of the source mass, and $d^3\vec{r}'$ is a three-dimensional volume element at $\vec{r}'$ of the source mass. Along the most significant direction, B' induced by the rotating source masses can be expanded in a Fourier series as

$$B'(t) = c_0 + \sum_{n=1}^{\infty} c_n \cos(n\omega_0 t + \phi),$$

where c_n is the Fourier coefficient and ϕ the initial phase factor. In the experiment, when taking into account the noise, the detected signal is

$$B_{\mathrm{exp}}(t) = \alpha c_0 + \alpha \sum_{n=1}^{\infty} c_n \cos(n\omega_0 t + \phi) + n(t),$$

where $\alpha = g_V g_A$ for the VA interaction and $\alpha = g_A^2$ for the AA interaction respectively, and $n(t)$ is the measurement noise. For each harmonic component, the coupling constant α can be derived as

$$\alpha|_n = \frac{2\int_0^{NT} \cos(n\omega_0 t + \phi) B_{\mathrm{exp}}(t) dt}{c_n NT} \tag{3}$$

where N is an integer, $T = 1/f_0$ is the period of the modulated signal, $\omega_0 = 2\pi f_0$ is the modulating frequency, and NT is the total observing time. According to the Fourier expansion of $B'(t)$, harmonic terms from one to four using weighted mean can determine α [39]. The noise contribution can be estimated as [40]

$$\delta\bar{\alpha}|_{\mathrm{noise}} \sim \sqrt{S_N(nf_0)}\sqrt{\frac{2}{NT}}\frac{1}{\sqrt{\sum_{n=1}^{4} c_n^2}}, \tag{4}$$

where $S_N(nf_0)$ is the noise power density at the corresponding harmonic frequency. In this Letter, we found that $S_N(nf_0)$ for a single AM is approximately at a constant level of $\sim$20 fT/$\sqrt{\mathrm{Hz}}$ for the harmonic frequencies of interest. The DC term is not used to avoid the $1/f$ noise of the AMs. Using the most significant harmonics in the weighted average could further increase the SNR, as can be seen from Eq. (4). Furthermore, four identical AMs arranged in an array are used to improve the statistics and reduce the common-mode noise.

The experimental setup.—The experimental setup is shown in Fig. 1. Two identical BGO ($Bi_4Ge_3O_{12}$) crystal cylinders with both a diameter and length of 10.16 cm are attached to the rotating shaft of a high-power servo motor. The BGO crystals containing impurities of less than 1 ppm have a high mass density (7.13 g/cm^{-3}), thus a high number density of nucleons (4.26×10^{24} cm^{-3}) and very low magnetic susceptibility (-19.0×10^{-6}) [41]. All these features make the crystal a good choice as the source masses

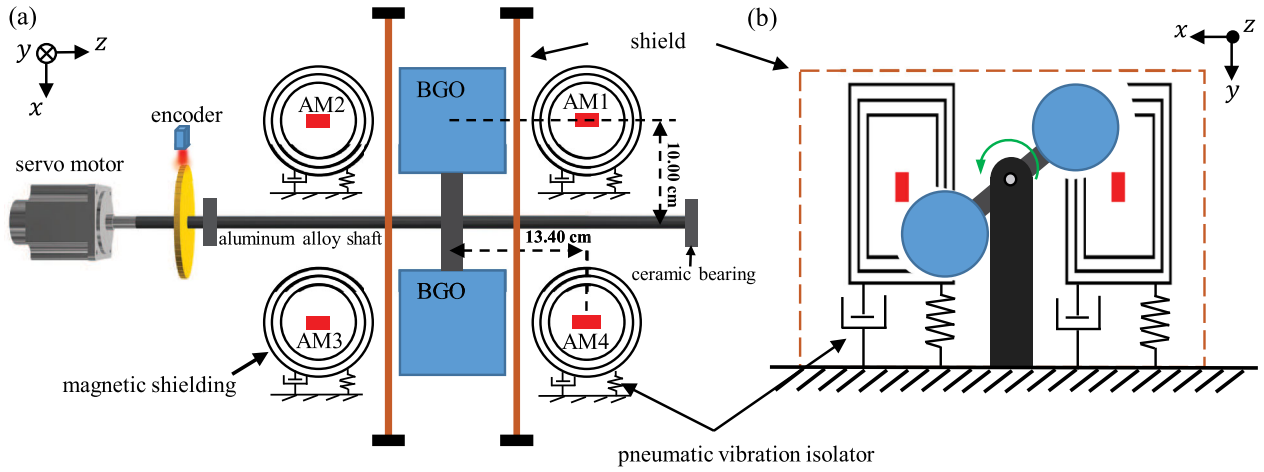

FIG. 1. Schematic of the experimental setup. (a),(b) The top and end views of the setup, respectively. The servo motor rotates the two BGO cylinders as source masses which have a modulating frequency of 20 Hz, inducing pseudomagnetic field signals to the surrounding AMs if exotic spin- and velocity-dependent interactions exist. The AMs are magnetically shielded and placed on a platform sitting on pneumatic vibration isolators. A 1 cm thick aluminum plate shielding is applied to prevent possible air vibration caused by the rotating source masses. The encoder monitors the rotating angle and frequency in real time.

for searching for the exotic spin-dependent interactions [25,26,42]. The 4-inch diameter BGO crystals are the largest we could find [43]. The mass of a single BGO crystal is 5.87 Kg which is the largest crystal ever used in the new interaction searching experiment, to the best of our knowledge. In comparision, Refs. [25,26,42,44] used BGO crystals with masses of ∼100 g. The shaft material is chosen to be an aluminum alloy of 7475, which is strong and has a lower magnetic susceptibility than the common 6xxx series alloys. We also carefully chose the ceramic bearings to support the rotating shaft. The servo motor rotates the two crystals at a frequency of ∼10 Hz; thus, the source masses are rotationally modulated at a frequency of ∼20 Hz. A fiber-optic encoder is applied to monitor the precise rotating angle and frequency in real time.

An array of four identical, high sensitivity, commercially available AMs is used to detect the new interactions. The AMs of model QZFM Gen-3, made by QuSpin Inc., are compact in size (sensor dimensions: $12.4 \times 16.6 \times 24.4$ mm) and have typical sensitivity of 7–10 $\mathrm{fT}/\sqrt{\mathrm{Hz}}$ [45]. Each AM is placed inside a magnetic shielding which has an outer diameter of 12 cm and length of 28 cm and is made of 3 layers of permalloy. The magnetic shielding provides a magnetic environment with a residual field level of $< \sim 5$ nT; thus, the AMs can work at their best sensitivities. In practice, Johnson noise from the shielding metal will make extra contributions, worsening the sensitivity. We observed 20 $\mathrm{fT}/\sqrt{\mathrm{Hz}}$ using the magnetic shielding in this work. The magnetic shielding can screen possible magnetic noise, which will disturb the polarized electron spin inside the shielding. At the same time, the exotic spin-dependent interactions will not be affected since the pseudomagnetic field it induced is not subject to Maxwell's equations [7,46]. The AMs have a bandwidth of 200 Hz, which is good enough since the highest harmonic frequency under consideration is ∼80 Hz.

The exotic spin-dependent interactions due to the source masses, if they exist, can induce pseudomagnetic field signals for the polarized electron spin of the surrounding AMs. The AMs are dual axis and can be set to be sensitive to either the $\hat{x}$ or $\hat{y}$ direction in our setup as shown in Fig. 1. To detect the VA type of interaction, the AMs are set to measure along the $\hat{y}$ direction, and the signal due to the new interaction can be extracted as

$$B_{\mathrm{exp}} = \frac{1}{4}(-B_1 - B_2 + B_3 + B_4), \tag{5}$$

where B_i is the magnetic field sensed by sensor AM_i. When the source masses are rotating clockwise, obviously, any common noises that get added to the signals can be canceled. In practice, the performance difference of the magnetic shieldings, which can induce different responses of the AMs, has to be taken into account. In this case, we could cancel more common-mode noise by carefully arranging shieldings, e.g., we could use the best and the worst shieldings for AM1 and AM2, and the other two for the rest of the AMs; thus, the nonuniformity effects can be mostly canceled. We performed tests applying a common ac field to the AMs inside the magnetic shieldings and found more than 90% of the common-mode noise can be canceled by this method. A data-taking example of this configuration is shown in Fig. 2. When searching for the AA type of new interaction, the AMs are set to be sensitive in the $\hat{x}$ direction, and the new interaction signal can be extracted as

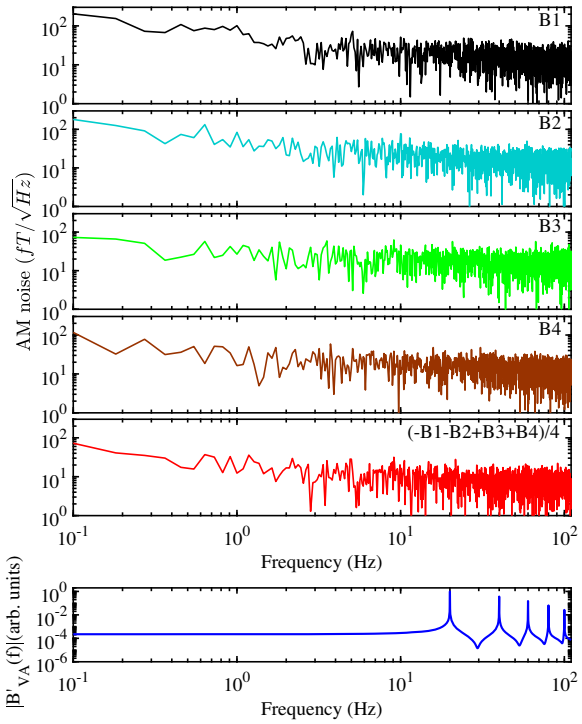

FIG. 2. Noise-power-density measurement examples of the VA searching setup. B_i is the magnetic field sensed by sensor AM_i. $B_{\mathrm{exp}} = (-B_1 - B_2 + B_3 + B_4)/4$ is plotted for the VA setup. The bottom plot is the Fourier transformation of the simulated signal B'_{VA}.

$$B_{\mathrm{exp}} = \frac{1}{4}(-B_1 + B_2 - B_3 + B_4) \tag{6}$$

when rotating clockwise.

Since two heavy source masses are rotating at a speed of 600 RPM, one of the main challenges of the experiment is to isolate the vibrations effectively. The AMs, cables, electronics, and other necessary parts are placed on a pneumatic vibration-isolation platform (Newport S-2000AN nonmagnetic pneumatic vibration isolators and the M-RPR-N nonmagnetic optical table) with a vertical resonance frequency of 1 Hz and horizontal resonance frequency of 1.5 Hz.Although the 10 Hz vibration can still be seen on some AMs as in Fig. 2, it shows no presence on the harmonic frequencies of interest of 20, 40, 60, and 80 Hz. Furthermore, shielding made of aluminum plate with 1-cm thickness is implemented to prevent possible air vibration [44], which is also caused by the rotations of the heavy masses and might disturb the AMs. Closed cable trunking is used to shield all the necessary parts of the connecting cables. To further reduce the noise, the AMs are powered by a UPS, and the 50 Hz peak of the line power is not seen as in our previous measurement (Fig. 2 of Ref. [39]).

A digital, multichannel data acquisition card (DAQ) with a maximum sampling rate of 2 MHz is used to read the output signals of the encoder and AMs synchronously. The data-taking cycles are as follows. The source masses were first rotated clockwise for 660 s, then counterclockwise for the same amount of time. Each 660 s cycle is further divided into 60 segments of length 11 s to avoid overstacking the DAQ card. When reversing the rotation direction, the signal due to the new interaction changes its sign, while noises that do not change can be rejected. For the VA type of interaction searching, the total data integration time is 130 h, and for AA, 243 h.

Data processing and results.—The data processing procedure is as follows. For each data segment of 11 s, the rotating or the modulating frequency f_0 is obtained with a typical error of $\sim 1.5 \times 10^{-4}$ Hz by fitting the time series from the Phase A signal of the encoder. Then the period T of the modulated signal can be calculated. The 11 s data segment can be truncated to be an integer number of the period to avoid unnecessary uncertainties for performing the integrations. The initial phase of the system can be determined with a typical error of 0.024° using the Phase C signal from the encoder. With the known ω_0 and ϕ, $B'(t)$ can be calculated using Monte Carlo techniques as in Refs. [25–27]. Then c_n can be obtained by numerically integrating. Once c_n is obtained, α, or $g_V g_A$ and $g_A g_A$ can be calculated by the integration of Eq. (4) using the $B_{\mathrm{exp}}(t)$ time series measured by the AMs. Simpson's method, which is a numerical integration technique with high precision [47], is applied throughout the work. Once α and $-\alpha$ are obtained for each clockwise and counterclockwise cycle, the $[+1, -3, +3, -1]$ weighting method [25,26,48] is applied to remove possible slow drifting of the system further [49]. Furthermore, by flipping the signal of interest at a specific frequency, the method could also cancel noise significantly [50].

Errors due to uncertainties of f_0, ϕ, rotation radius, the distance between AMs and the source masses, contributions from the rotating aluminum parts, etc., were carefully analyzed. The systematic errors were only a few percent of the statistics. Our main results are shown in Figs. 3 and 4. For $\lambda = 10$ m, we obtained

$$g_V^N g_A^e = 0.07 \pm 2.06(\mathrm{stat}) \pm 0.07(\mathrm{syst}) \times 10^{-34}, \tag{7}$$

$$g_A^N g_A^e = -0.06 \pm 2.36(\mathrm{stat}) \pm 0.08(\mathrm{syst}) \times 10^{-22}. \tag{8}$$

Conclusion and discussion.—The experimental scheme proposed previously in Ref. [39] for searching for VA and AA types of new interactions was realized in this Letter. As shown in Figs. 3 and 4, in the interaction range from ~0.2 m to 10 m, the present results improve the limits on $|g_V^N g_A^e|$ by ~20 000 times and on $|g_A^N g_A^e|$ by ~140 times. The major source of systematic errors for the experiment would come from the vibrations caused by the high-speed rotation of the heavy source masses. We successfully circumvented

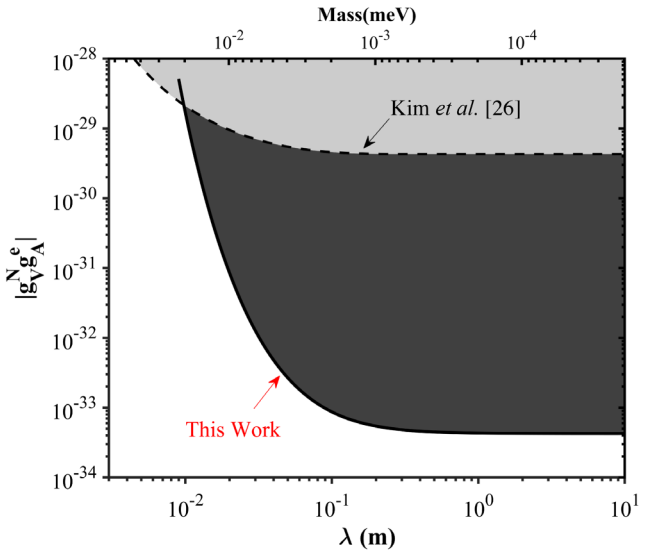

FIG. 3. Constraints on the coupling constants $|g_V^N g_A^e|$ (1σ) as a function of interaction range λ and new boson mass. The dashed line is from Ref. [26]. The solid line (dark area) is the present work.

it by using the pneumatic vibration isolation techniques. To further improve the sensitivity of the experiment method described in this Letter, one way is to reduce the noise of the AMs. ~ 20 fT$/\sqrt{\text{Hz}}$ noise level was measured in this Letter when placing a single AM inside the small magnetic shielding (inner diameter of 60 mm and length of 208 mm) used in this work. ~ 10 fT$/\sqrt{\text{Hz}}$ noise level has been observed [39] when using a much larger magnetic shielding (with an inner diameter of 400 mm and length of 800 mm).

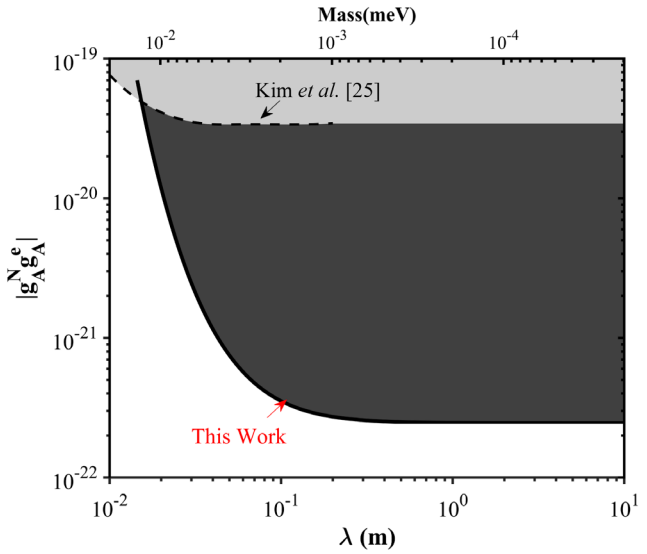

FIG. 4. Constraints on the coupling constants $|g_A^N g_A^e|$ (1σ) as a function of interaction range λ and new boson mass. The dashed line is from Ref. [25]. The solid line (dark area) is the present work.

It would not be easy to arrange the experiment with source masses and AMs inside the shielding to avoid systematics caused by the vibrations and air currents, especially the latter. However, it is possible to put the whole system inside a rough vacuum to solve the problem. Thus, firstly, we can avoid the systematics caused by the air vibrations; secondly, we can improve the AMs' sensitivity; thirdly, we can reduce the distance between the AMs and the source mass surfaces to the mm scale. These possible improvements can result in better sensitivity, but it is more challenging to carry out the experiment.

We acknowledge support from the National Natural Science Foundation of China (Grant No. U2030209). This work was also supported by the National Key Program for Research and Development of China under Grants No. 2020YFA0406001 and No. 2020YFA0406002. We thank Chongqing Medical University for the loan of the AMs. We thank Dr. W. Ji, H. F. Dong, D. Sheng, and H. Yuan for helpful discussions. We thank Dr. GouZei and Y. Lan for proofreading the manuscript. We thank the anonymous referees for inspiring comments and suggestions.

*Corresponding author.
hyan@caep.cn

[1] P. Sikivie, Invisible axion search methods, Rev. Mod. Phys, **93**, 015004 (2021).
[2] P. A. Zyla, R. M. Barnett, J. Beringer, O. Dahl *et al.*, Review of particle physics, Prog. Theor. Exp. Phys. **2020**, 083C01 (2020).
[3] R. D. Peccei and H. R. Quinn, CP Conservation in the Presence of Pseudoparticles, Phys. Rev. Lett. **38**, 1440 (1977).
[4] F. Wilczek, Problem of Strong P and T invariance in the Presence of Instantons, Phys. Rev. Lett. **40**, 279 (1978).
[5] S. Weinberg, A New Light Boson?, Phys. Rev. Lett. **40**, 223 (1978).
[6] J. E. Moody and F. Wilczek, New macroscopic forces?, Phys. Rev. D **30**, 130 (1984).
[7] A. Arvanitaki and A. A Geraci, Resonantly Detecting Axion-Mediated Forces with Nuclear Magnetic Resonance, Phys. Rev. Lett. **113**, 161801 (2014).
[8] W. A. Terrano, E. G. Adelberger, J. G. Lee, and B. R. Heckel, Short-range, Spin-dependent Interactions of Electrons: A Probe for Exotic Pseudo-goldstone Bosons, Phys. Rev. Lett. **115**, 201801 (2015).
[9] N. Crescini, C. Braggio, G. Carugno, P. Falferi, A. Ortolan, and G. Ruoso, Improved constraints on monopole dipole interaction mediated by pseudo-scalar bosons, Phys. Lett. B **773**, 677 (2017).
[10] J. Y. Lee, A. Almasi, and M. Romalis, Improved Limits on Spin-mass Interactions, Phys. Rev. Lett. **120**, 161801 (2018).
[11] A. A. Geraci, G. Rybka, and K. van Bibber, Progress on the ARIADNE axion experiment, Springer Proc. Phys. **211**, 151 (2018), https://link.springer.com/chapter/10.1007/978-3-319-92726-8_18.

[12] Nancy Aggarwal *et al.* (the ARIADNE Collaboration), Characterization of magnetic field noise in the ARIADNE source mass rotor, Phys. Rev. Research **4**, 013090 (2022).
[13] N. Crescini, G. Carugno, P. Falferi, A. Ortolan, G. Ruoso, and C. C. Speake, Search of spin-dependent fifth forces with precision magnetometry, Phys. Rev. D **105**, 022007 (2022).
[14] B. A. Dobrescu and I. Mocioiu, Spin-dependent macroscopic forces from new particle exchange, J. High Energy Phys. 11 (2006) 005.
[15] B. Holdom, Two U(1)'s and charge shifts, Phys. Lett. **166B**, 196 (1986).
[16] B. A. Dobrescu, Massless gauge bosons other than the photon, Phys. Rev. Lett. **94**, 151802 (2005).
[17] D. Atwood, C. P. Burgess, E. Filotas, F. Leblond, D. London, and I. Maksymyk, Supersymmetric large extra dimensions are small and/or numerous, Phys. Rev. D **63**, 025007 (2000).
[18] P. C. Malta, L. P. R. Ospedal, K. Veiga, and J. A. Helayl-Neto, Comparative aspects of spin-dependent interaction potentials for spin-1/2 and spin-1 matter fields, Adv. High Energy Phys. **2016**, 2531436 (2016).
[19] P. Fadeev, New gauge bosons and where to find them, M.S. dissertation of Ludwig Maximilian University of Munich, 2018.
[20] P. Fadeev, Y. V. Stadnik, F. F, Mikhail G. Kozlov, V. V. Flambaum, and D. Budker, Revisiting spin-dependent forces mediated by new bosons: Potentials in the coordinate-space representation for macroscopic- and atomic-scale experiments, Phys. Rev. A **99**, 022113 (2019).
[21] H. Yan, G. A. Sun, S. M. Peng, Y. Zhang, C. Fu, H. Guo, and B. Q. Liu, Searching for New Spin- and Velocity-dependent Interactions by Spin Relaxation of Polarized He3 Gas, Phys. Rev. Lett. **115**, 182001 (2015).
[22] H. Yan and W. M. Snow, New Limit on Possible Long-Range Parity-Odd Interactions of the Neutron from Neutron-Spin Rotation in Liquid ^4He, Phys. Rev. Lett. **110**, 082003 (2013).
[23] T. M. Leslie, E. Weisman, R. Khatiwada, and J. C. Long, Prospects for electron spin-dependent short-range force experiments with rare earth iron garnet test masses, Phys. Rev. D **89**, 114022 (2014).
[24] J. Ding, J. Wang, X. Zhou, Y. Liu, K. Sun, A. O. Adeyeye, H. Fu, X. Ren, S. Li, P. Luo, Z. Lan, S. Yang, and J. Luo, Constraints on the Velocity and Spin Dependent Exotic Interaction at the Micrometer Range, Phys. Rev. Lett. **124**, 161801 (2020).
[25] Y. J. Kim, P. H. Chu, and I. Savukov, Experimental Constraint on an Exotic Spin- and Velocity-dependent Interaction in the sub-meV Range of Axion Mass with a Spin-Exchange Relaxation-Free Magnetometer, Phys. Rev. Lett. **121**, 091802 (2018).
[26] Y. J. Kim, P. H. Chu, I. Savukov, and S. Newman, Experimental limit on an exotic parity-odd spin- and velocity-dependent interaction using an optically polarized vapor, Nat. Commun. **10**, 2245 (2019).
[27] W. Ji, Y. Chen, C. Fu, M. Ding, J. Fang, Z. Xiao, K. Wei, and H. Yan, New Experimental Limits on Exotic Spin-spin-velocity-dependent Interactions by Using $SmCo_5$ Spin Sources, Phys. Rev. Lett. **121**, 261803 (2018).
[28] F. M. Piegsa and G. Pignol, Limits on the Axial Coupling Constant of New Light Bosons, Phys. Rev. Lett. **108**, 181801 (2012).
[29] F. Ficek, D. Kimball, M. G. Kozlov, N. Leefer, S. Pustelny, and D. Budker, Constraints on exotic spin-dependent interactions between electrons from helium fine-structure spectroscopy, Phys. Rev. A **95**, 032505 (2017).
[30] F. Ficek, P. Fadeev, V. V. Flambaum, D. Kimball, M. G. Kozlov, V. Stadnik, Yevgeny, and D. Budker, Constraints on Exotic Spin-Dependent Interactions Between Matter and Antimatter from Antiprotonic Helium Spectroscopy, Phys. Rev. Lett. **120**, 183002 (2018).
[31] H. Yan, G. A. Sun, S. M. Peng, H. Guo, B. Q. Liu, M. Peng, and H. Zheng, Constraining exotic spin dependent interactions of muons and electrons, Eur. Phys. J. C **79**, 971 (2019).
[32] M. Safronova, D. Budker, D. DeMille, D. F. J. Kimball, A. Derevianko, and C. W. Clark, Search for new physics with atoms and molecules, Rev. Mod. Phys. **90**, 025008 (2018).
[33] I. K. Kominis, T. W. Kornack, J. C. Allred, and M. V. Romalis, A subfemtotesla multichannel atomic magnetometer, Nature (London) **422**, 596 (2003).
[34] D. Budker and D. F. Kimball, *Optical Magnetometry* (Cambridge University Press, Cambridge, England, 2013).
[35] P. H. Chu, Y. J. Kim, and I. Savukov, Search for exotic spin-dependent interactions with a spin-exchange relaxation-free magnetometer, Phys. Rev. D **94**, 036002 (2016).
[36] E. Boto, N. Holmes, J. Leggett, G. Roberts, S. S. Meyer, L. D. Munõz, K. J. Mullinger, T. M. Tierney, S. Bestmann, G. R. Barnes, R. Bowtell, and M. J. Brookes, Moving magnetoencephalography towards real-world applications with a wearable system, Nature (London) **555**, 657 (2018).
[37] E. Boto, R. M. Hill, M. Rea, N. Holmes, Z. A. Seedat, J. Leggett, V. Shah, J. Osborne, Richard Bowtell, and M. J. Brookes, Measuring functional connectivity with wearable MEG, NeuroImage **230**, 117815 (2021).
[38] M. Rea, N. Holmes, R. M. Hill, E. Boto, J. Leggett, L. J. Edwards, D. Woolger, E. Dawson, V. Shah, J. Osborne, R. Bowtell, and M. J. Brookes, Precision magnetic field modeling and control for wearable magnetoencephalography, NeuroImage **241**, 118401 (2021).
[39] K. Wu, S. Chen, M. Peng, J. Gong, and H. Yan, Searching for exotic spin-dependent interactions using rotationally modulated source masses and an atomic magnetometer array, Phys. Rev. D **105**, 055020 (2022).
[40] K. G. Libbrecht, E. D. Black, and C. M. Hirata, A basic lock-in amplifier experiment for the undergraduate Laboratory, Am. J. Phys. **71**, 1208 (2003).
[41] S. Yamamoto, K. Kuroda, and M. Senda, Scintillator selection for MR-compatible gamma detectors, IEEE Nucl. Sci. **50**, 1683 (2003).
[42] K. Tullney, F. Allmendinger, M. Burghoff, W. Heil, S. Karpuk, W. Kilian, S. Knappe-Grüneberg, W. Müller, U. Schmidt, A. Schnabel, F. Seifert, Y. Sobolev, and L. Trahms, Constraints on Spin-dependent Short-range Interaction between Nucleons, Phys. Rev. Lett. **111**, 100801 (2013).
[43] http://www.siccas.com/BGOCrystalscintillatorBismuthgermanate.htm.

[44] H. W. Su, Y. H. Wang, M. Jiang, W. Ji, P. Fadeev, D. H. Hu, X. H. Peng, and D. Budker, Search for exotic spin-dependent interactions with a spin-based amplifier, Sci. Adv. **7**, eabi9535 (2021).

[45] QuSpin Inc., Available at: https://quspin.com/products-qzfm/.

[46] I. Antoniadis, S. Baessler, M. Bchner, V. V. Fedorov, S. Hoedl, A. Lambrechti, V. V. Nesvizhevsky, G. Pignol, K. V. Protasov, S. Reynaud, and Yu. Sobolev, Short-range fundamental forces, C.R. Phys. **12**, 755 (2011).

[47] H. Yan, K. Li, R. Khatiwada, E. Smith, W. M. Snow, C. B. Fu, P.-H. Chu, H. Gao, and W. Zheng, A frequency determination method for digitized NMR signals, Comput. Phys. Commun. **15**, 1343 (2014).

[48] P. H. Chu, A. Dennis, C. B. Fu, H. Gao, R. Khatiwada, G. Laskaris, K. Li, E. Smith, W. M. Snow, H. Yan, and W. Zhang, Laboratory search for spin-dependent short-range force from axion-like-particles using optically polarized 3He gas, Phys. Rev. D **87**, 011105(R) (2013).

[49] A brief description of the weighting method is as follows [48]. Suppose there are time-dependent quadratic drifts for the system, then the measured signal can be expressed as:

$$B_{exp}(t) = at^2 + bt + c \pm B' \tag{9}$$

where a,b,c are constants describing the slow drifting, t is time and $+B'(-B')$ the signal of interest when the system is rotating CW(CCW). We make a serial of alternating CW/CCW measurements with time-interval ΔT; thus, we have a time series as $B_{exp}(\Delta T)(CW)$, $B_{exp}(2\Delta T)(CCW)$, $B_{exp}(3\Delta T)(CW)$, $B_{exp}(4\Delta T)(CCW)$…. Simply subtracting the CW signal by CCW can only remove the constant term of the drifting completely. It is easy to see that when doing the so-called $[+1, -3, +3, -1]$ weighting average, we can extract the signal as:

$$B' = \frac{1}{8}[B_{exp}(\Delta T)(CW) - 3B_{exp}(2\Delta T)(CCW) + 3B_{exp}(3\Delta T)(CW) - B_{exp}(4\Delta T)(CCW)]$$

This method can remove the slow drifting up to the quadratic terms, which is usually good enough for precision measurements.

[50] W. M. Snow, C. D. Bass, T. D. Bass, B. E. Crawford, K. Gan, B. R. Heckel, D. Luo, D. M. Markoff, A. M. Micherdzinska, H. P. Mumm, J. S. Nico, A. K. Opper, M. Sarsour, E. I. Sharapov, H. E. Swanson, S. B. Walbridge, and V. Zhumabekova, Upper bound on parity-violating neutron spin rotation in ^{4}He, Phys. Rev. C **83**, 022501(R) (2011).